BMB
Reports

BMB Rep. 2023; 56(11): 606-611
www.bmbreports.org

The N-terminal peptide of the main protease of SARS-CoV-2, targeting dimer interface, inhibits its proteolytic activity

Sunyu Song[1,#], Yeseul Kim[1,#], Kiwoong Kwak[1], Hyeonmin Lee[1], Hyunjae Park[1], Young Bong Kim[2], Hee-Jung Lee[2] & Lin-Woo Kang[1,]*

[1]Department of Biological Sciences, Konkuk University, Seoul 05029, [2]Department of Biomedical Science and Engineering, Konkuk University, Seoul 05029, Korea

The main protease (Mpro) of SARS-CoV-2 cleaves 11 sites of viral polypeptide chains and generates essential non-structural proteins for viral replication. Mpro is an important drug target against COVID-19. In this study, we developed a real-time fluorometric turn-on assay system to evaluate Mpro proteolytic activity for a substrate peptide between NSP4 and NSP5. It produced reproducible and reliable results suitable for HTS inhibitor assays. Thus far, most inhibitors against Mpro target the active site for substrate binding. Mpro exists as a dimer, which is essential for its activity. We investigated the potential of the Mpro dimer interface to act as a drug target. The dimer interface is formed of domain II and domain III of each protomer, in which N-terminal ten amino acids of the domain I are bound in the middle as a sandwich. The N-terminal part provides approximately 39% of the dimer interface between two protomers. In the real-time fluorometric turn-on assay system, peptides of the N-terminal ten amino acids, N10, can inhibit the Mpro activity. The dimer interface could be a prospective drug target against Mpro. The N-terminal sequence can help develop a potential inhibitor. [BMB Reports 2023; 56(11): 606-611]

INTRODUCTION

The Coronaviridea family is genetically classified into four groups: α-coronaviruses, β-coronaviruses (which are further classified into four distinct viral lineages from A to D), γ-coronaviruses, and δ-coronaviruses (1). Following occurrences of Severe Acute Respiratory Syndrome (SARS) in 2002 and Middle East Respiratory Syndrome (MERS) in 2012, SARS-CoV-2, the most pathogenic β-coronavirus, was first reported in Wuhan, China, in December 2019 (2-5). On January 31, 2020, the World Health Organization (WHO) officially designated the disease caused by SARS-CoV-2 as COVID-19 and declared it a pandemic on March 11, 2020 (6, 7).

Like other coronaviruses, SARS-CoV-2 is an enveloped virus with a large single-stranded RNA genome of approximately 30 kilobases. In the genome, four structural proteins and two polyproteins (pp1a and pp1ab) encompass all essential viral proteins required for invading host cells and ensuring the continuity of the viral life cycle (8, 9). The genome of SARS-CoV-2 shares 79% sequence identities with that of SARS and 50% sequence identities with that of MERS (10, 11).

By interacting with surface glycoprotein S and ACE2 receptor of host cells, SARS-CoV-2 can enter the cellular environment (12). The giant positive genomic RNA can interact with the host's ribosome and translate into two polyproteins (pp1a and pp1ab) consisting of NSP1-11 and NSP1-16 (13). The polyprotein matures into smaller Non-Structural Proteins (NSPs) through viral proteolysis by two cysteine proteases of the Main protease (Mpro) or 3C-like protease (3CLpro) and the papain-like protease (PLpro) (14, 15).

Inhibition of Mpro activity can interrupt the replication of SARS-CoV-2 (16). The dissimilarity of SARS-CoV-2 Mpro from human proteases makes it a prospective drug target for small molecule drugs against SARS-CoV-2 (14). Since the sequence and structure of the SARS-CoV-2 Mpro are closely related to those from other β-coronaviruses, many previously developed inhibitors have been tried as lead compounds for SARS-CoV-2 Mpro (17, 18).

Mpro is known to be active as a dimer, in which only a protomer is active at a time (19). In the monomer conformation, conformation change of S139 to L141 part can block the substrate binding pocket (20). Mutation and deletion studies of the N-terminal part important for dimerization have shown very low or no catalytic activity in a monomer conformation (21).

*Corresponding author. Tel: +82-2-450-4090; Fax: +82-2-444-6707; E-mail: lkang@konkuk.ac.kr
#These authors contributed equally to this work.

https://doi.org/10.5483/BMBRep.2023-0153

Received 21 August 2023, Revised 6 September 2023, Accepted 20 September 2023, Published online 19 October 2023

Keywords: Dimerization, Drug discovery, Inhibitor screening, Main protease, SARS-CoV-2

ISSN: 1976-670X (electronic edition)

RESULTS

Mpro purification

Mpro was induced and expressed for 16 h at 288 K for soluble protein expression. Expressed Mpro proteins were sequentially purified via Ni-NTA affinity and size exclusion chromatography. His-affinity tag was cleaved in the middle of purification. Resulting affinity tag-free Mpro proteins were purified as shown in SDS-page (Fig. 1A). Analytical size exclusion chromatography confirmed that the purified Mpro showed a dimer conformation as previously published (Fig. 1B and Supplementary Fig. 1) (20). Purified Mpro proteins were concentrated to 5 mg/ml and stored at 193 K for further usage.

Real-time fluorometric turn-on assay system

A real-time fluorometric turn-on assay system was set up to measure the proteolytic activity of Mpro (Fig. 1C). It is known that SARS-CoV Mpro cleaves the site between NSP4 and NSP5 most effectively (22). The SARS-CoV-2 Mpro shares 96% sequence identity with SARS-CoV Mpro. The peptide of EKTSAVLQ/SGFRKMAKS between NSP4 and NSP5, with "/" indicating the proteolytic cleavage position, was used as a substrate in the FRET assay system. The fluorophore of Edans was attached to the N-terminus of the peptide. The quencher of Dabcyl was the C-terminus. In the intact substrate, the light of 360 nm excited the Edans fluorophore and the nearby Dabcyl quencher blocked the emission from the excited Edan fluorophore. When Mpro cleaved the substrate, the quencher was released away from the excited fluorophore and fluorescence was emitted at 460 nm.

The real-time fluorometric turn-on assay showed that Mpro cleaved substrate peptides efficiently in a concentration-dependent manner (Fig. 1D). When we measured Mpro activity with increasing concentrations of fluorogenic substrates, the emitted fluorescence was proportionally increased. The slope of fluorescence signals showed initial proteolytic velocities at each substrate concentration. It was linear for up to 60 mins. Fluorescence signals reached plateaus approximately in 180 mins. Triplicated assays showed that measured activities were reproducible. Frozen aliquots of the purified Mpro and substrates produced reproducible catalytic activities in the developed assay system, which would be helpful for HTS assays. In the assay, the negative control was incubated without Mpro, which showed no fluorescence. The basal level decreased over 4 hours. The negative control showed a slowly decreasing fluorescence signal.

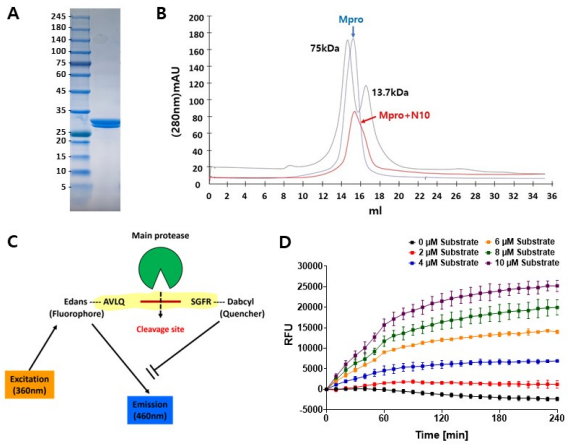

Fig. 1. The real-time fluorometric turn-on assay system of the proteolytic activity of Mpro. (A) Purified Mpro proteins in SDS-page. The purified Mpro proteins of 33.8 kDa are shown in SDS-PAGE. (B) Size exclusion chromatography of Mpro alone (blue) and supplemented with N10 (red). The conalbumin of 75 kDa (Cytiva, USA) and the ribonuclease A of 13.7 kDa (Cytiva, USA) are used as molecular weight standards (black). (C) Scheme of the real-time fluorometric turn-on assay system of Mpro. The Mpro is shown in green, and excitation and emission of fluorescence are shown in orange and blue, respectively. (D) Substrate concentration-dependent Mpro activity in the real-time fluorometric turn-on assay system. Mpro shows the proportional increasing proteolytic activity in the assay system depending on the substrate concentration up to 10 μM.

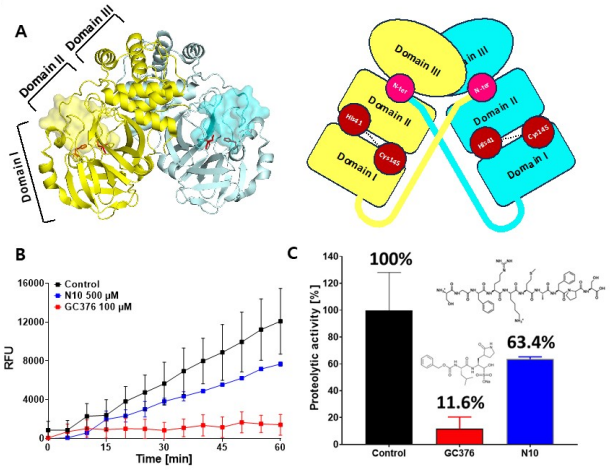

Fig. 2. The inhibition of Mpro activity by the N-terminal ten amino acids peptide N10. (A) The crystal structure of Mpro dimer. Two protomers in the dimer are shown in yellow and cyan. A protomer consists of three domains of I, II, and III. The active site of Mpro exists in the crevice between domain I and II, as shown with the surface presentation. The N-terminal end of each protomer is bound in the crevice between domain II and III of the other protomer. The N-terminals are shown in magenta circles. The catalytic residues of Cys145 and His41 are shown in red. (B) The inhibition of Mpro activity of GC376 and N10. GC376, as a positive control of the Mpro inhibitor, almost completely inhibits the Mpro activity, and N10 also shows inhibitory activity in the real-time fluorometric turn-on assay system. (C) Chemical structures of GC376 and N10 and the inhibitory effects. In the assay, 100 μM GC376 inhibits Mpro activity by 89% and 500 μM N10 by 37%.

Table 1. Interacting surface area of N10 in Mpro dimer

Target molecule: N10 of protomer A	Area (Å^2)	Percentage (%) in total surface area
Total solvent accessible surface	1,653	100.0
Interaction surface with protomer B	565	34.2
Interaction surface with protomer A	837	50.6
Solvent accessible surface in Mpro dimer	251	15.2

Mpro inhibition of GC376

GC376, a prodrug of GC373, is a well-known peptidomimetic inhibitor against both SARS-CoV and SARS-CoV-2 Mpro enzymes (23, 24). It had a nanomolar range inhibitory activity against both Mpro enzymes. In the real-time fluorometric turn-on assay system, GC376 at 100 μM concentration resulted in almost complete inhibition (Fig. 2 and Supplementary Fig. 2). This result confirms that the developed real-time fluorometric turn-on assay system is reliable and consistent with previous publications (25).

Dimer interaction surface of Mpro

The dimer conformation of Mpro is essential for its activity (17, 26). Interaction surface areas between Mpro protomers were calculated from the crystal structure of Mpro (Table 1). In the dimer conformation, two protomers are bound to each other, mainly based on domains II and III (Fig. 2A and Supplementary Fig. 3), in which the N-terminal ten amino acids (N10) of domain I extends into the center of the dimer interface (Fig. 3A, B). The dimer interaction area between protomers A and B was 1,431Å^2. Approximately 10% of the total surface area of protomer A (14,251Å^2) was involved in dimerization (Supplementary Table 1).

The total surface area was 1,653Å^2 for the N10 alone and 14,251Å^2 for the protomer A in the monomer form. The interaction area between N10 and the remaining part of protomer A was 837Å^2 and that between the N10 of protomer A and the intact protomer B was 565Å^2. In summary, N10 contributed to as much as 40% (565Å^2 out of 1,431Å^2) of the dimer interaction in terms of surface area. In addition, the dimer interaction surface of N10 occupied almost 34% (565Å^2 out of 1,653Å^2) of the total solvent-accessible surface of N10.

Activity inhibition by N-terminal peptide

Thus far, almost all Mpro inhibitors target the active site in the substrate-binding pocket. Based on the necessity of the dimer conformation for activity, the dimer interface was studied as a potential target site for inhibitor binding. The N-terminal part, especially the N10 sequence of SGFRKMAFPS, is located at the core of the dimer interaction. The peptide N10 was synthesized. It was soluble in water (Supplementary Fig. 4). The inhibitory activity of peptide N10 was measured in the Mpro assay

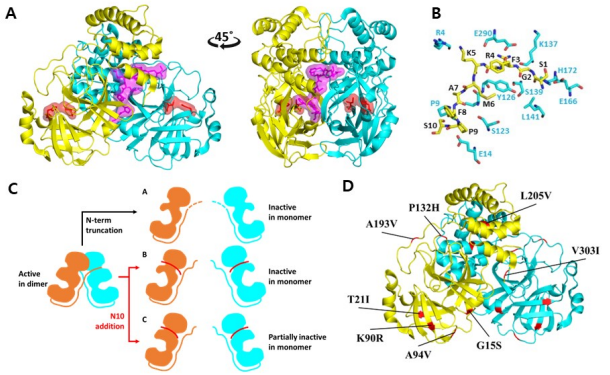

Fig. 3. The N-terminal ten amino acids in the Mpro dimer interface and the reported mutation sites in SARS-CoV-2 Mpro variants. (A) The N-terminal ten amino acids exist at the center of the dimer interface between two protomers. The N-terminal part of protomer A (yellow) is shown in purple with surface and the catalytic residues in the active site in red. (B) The enlarged view of the N-terminal part (yellow) bound in protomer B (cyan). (C) Potential inhibitory mechanisms of N10. Two protomers are shown in orange and cyan, in which the intact N-terminal part is shown as a solid line and the truncated part as a dashed line. The added N10 peptides are shown as a red line. (D) Mutated residues in SARS-CoV-2 Mpro variants. In 80 types of SARS-CoV-2 variants, eight residues were mutated and shown in red.

(Fig. 2B). At a concentration of 500 μM, N10 inhibited the Mpro activity approximately by 37% (Fig. 2C).

Disruption of dimer conformation by N-terminal peptide

To confirm that N10 could bind to the dimer interface and disrupt the dimerization, we performed analytical size exclusion chromatography of Mpro supplemented with N10. Adding N10 to Mpro shifted the Mpro dimer peak into a smaller size. The delayed shifted peak was half-size in height compared to the original peak. There was an overlapped shape of two peaks of primary and shoulder (Fig. 1B).

DISCUSSION

Viral proteases have been important drug targets. For example, in AIDS, HIV protease is a drug target for atazanavir sulfate (Reyataz), darunavir ethanolate (Prezista), fosamprenavir calcium (Lexiva), indinavir (Crixivan), lopinavir/ritonavir (Kaletra), nelfinavir (Viracept), ritonavir (Norvir), and saquinavir (Invirase) (27). Currently, for COVID-19, the FDA-approved lufotrelvir targets SARS-CoV-2 Mpro (28).

In this study, the dimer interface of Mpro was speculated as a potential drug target site. The area of the dimer interaction surface was calculated from the crystal structure, in which the N10 of the N-terminal ten amino acids was selected as a potent peptide molecule to inhibit Mpro activity. The ten amino acids peptide constitutes approximately 40% of the dimer in-

teraction surface. The truncated Mpro without the N-terminal four amino acids was changed to a monomer conformation with proteolytic activity lost (21, 29).

The inhibitory activity of N10 was weaker than that of GC376 in sub-millimolar concentrations (Fig. 2B). Adding N10 into Mpro changed the prospective conformation of Mpro from dimer to a smaller size, a presumably monomer. The singular symmetric peak of Mpro alone was changed to an overlapped uneven two peaks of primary and shoulder (Fig. 1B). Split peaks implied the heterogeneity of N10 bound Mpro proteins.

Previous studies have shown that the N-terminal amino acids are important for dimerization, which is essential for activity by maintaining the substrate-binding pocket in an active form (21). The weak inhibitory activity of N10 could be speculated in two ways (Fig. 3C). First, the binding affinity of N10 to Mpro protomer could not be high enough to shift an active dimer to an inactive monomer form. Alternatively, binding of the N10 peptide might shape the substrate-binding pocket as a partially active form mimicking that of the active dimer. The disappearing dimer peak in the size exclusion chromatography supported that N10 disrupted the dimer conformation. However, the heterogeneity of shifted peaks implied potentially interchangeable multiple conformations. If we could find a high-affinity compound to shift the active dimer to the inactive monomer, it would have a higher potential of a lead compound.

The dimer interface differs from the substrate binding pocket regarding availability. The substrate binding pocket is vacant without a substrate and available for inhibitor binding in apo status. In the case of the dimer interface, the other protomer could occupy the dimer interface. Therefore, the accessibility of the dimer interface could be a prerequisite. If dimer forms are in equilibrium with monomer forms, the dimer interface of monomer forms can be available for inhibitor binding and inhibitors could shift the equilibrium to the monomer conformation having no activity. Mpro is known to exist in equilibrium between dimer and monomer forms. The assay result showed that N10 could inhibit the proteolytic activity of Mpro, implying that the dimer interface could be a potential target site for developing a Mpro inhibitor. Residues involved in the dimer interface were not changed in representative SARS-CoV-2 variants (Fig. 3D and Supplementary Fig. 5), even with SARS-CoV or MERS (Supplementary Fig. 6) (30). The conserveness of the target site will increase the prospective value of the dimer interface inhibitor.

MATERIALS AND METHODS

Reagents

The expression host, *Escherichia coli* Rosetta™(DE3) pLysS, and the expression vector, pET29b, were purchased from Novagen (San Diego, CA, USA). All restriction enzymes were purchased from New England Biolabs (Hertfordshire, UK). The Luria-Bertani (LB) Broth (Lennox) medium and ampicillin were purchased from Sigma-Aldrich (Burlington, MA, United States).

Gene cloning

The gene encoding the Mpro protein from SARS-CoV-2 (isolate: Wuhan-Hu-1, nat-host: *Homo sapiens*, gene ID: 43740578) was synthesized based on the NCBI Website. The gene of Mpro was amplified using primers: forward primer 5′ CCCC CCATATGAGAGTGGTTTTAGAAAAATG 3′, and reverse primer 5′ GGGGGGCTCGAGTTACTTGGAAAGTAACACCTGA 3′, with the restriction enzyme sites of NdeI and XhoI at the 5′- and 3′-ends. The amplified DNA fragments were double-digested with the corresponding restriction enzymes and cloned into the pET29b-HT vector, which was modified to have additional residues of a 7 × His tag and a *Tobacco etch virus* (TEV) protease-cleavage site before the NdeI site in the pET29b vector (Novagen, USA).

Expression and purification of Mpro

The recombinant plasmid, pET29b-HT-Mpro, was transformed into *E. coli* Rosetta™(DE3) pLysS. Transformed *E. coli* Rosetta™ (DE3) pLysS cells were cultured at 310 K in LB medium supplemented with 100 μg/ml kanamycin antibiotics and induced at the exponential growth phase of an OD 600 nm of 0.5 with 0.1 mM isopropyl β-D-1-thiogalactopyranoside (IPTG). The culture was then incubated for a further 16 h at 288 K to express the Mpro. Cells were harvested by centrifugation at 5,000 × g using a Vision VS24-SMTi V506A rotor for 30 minutes at 277 K, resuspended with the A buffer (50 mM Tris-HCl pH 7.5, 300 mM NaCl, 15 mM imidazole, 20% glycerol, and 2 mM DTT), and disrupted using a sonicator (Korea process technology, Korea) on an ice bath.

The crude cell extract was centrifuged for 1 h at 15,000 × g using a Vision VS24-SMTi V508A rotor at 277 K to remove cell debris. To purify the 7 × His-tagged Mpro, the clarified supernatant was loaded onto a HisTrap HP resin (Cytivia, USA), equilibrated with the A buffer, and eluted with a gradient of 0 to 100% the B buffer (50 mM Tris-HCl pH 7.5, 500 mM NaCl, 500 mM imidazole, 20% glycerol, and 2 mM DTT). The eluate was dialyzed against the dialysis buffer (50 mM Tris-HCl pH 7.5, 300 mM NaCl, 20% glycerol, and 2 mM DTT) at 277 K for 4 h. The 7 × His-tag was removed using TEV protease at 277 K in an overnight reaction. Further purification was performed using a HisTrap HP column equilibrated in the A buffer. The Mpro was eluted with A buffer and further purified on the size-exclusion column (Superdex 75 16/600, GE Healthcare, Sonomasher) pre-equilibrated with the C buffer (50 mM Tris-HCl pH 7.5, 200 mM NaCl, 10% Glycerol, and 1 mM DTT). The Mpro was concentrated to 5 mg/ml using a centrifugal filter (Amicon Ultra-15, MWCO 10 kDa) and stored at 193 K.

Size exclusion chromatography for dimer confirmation

The molecular mass of Mpro was estimated by analytical size exclusion chromatography (SEC). The sample was applied onto the pre-equilibrated size-exclusion column (SuperoseTM-12 10/300, GE Healthcare, Sonomasher) and eluted at a 0.5 ml/min flow rate in buffer D (50 mM Tris-HCl pH 7.5, 1 M NaCl, 10%

Glycerol, and 1 mM DTT) at 298 K. The Conalbumin (Cytiva, USA) of Mr75000, and the Ribonuclease A (Cytiva, USA) of Mr13700 were used as molecular weight standards.

To calculate the molecular weight of eluted peaks, we draw the calibration graph. For drawing the calibration graph, we calculate the Kav of cocktail standards values by the following equation:

$$Kav = (Ve - Vo) / (Vc - Vo)$$

In the equation, Vo means the void volume: Vc, the accessible volume, and Ve, the analyte retention volume.

Fluorogenic substrate preparation for assay

The Mpro substrate #79952 (BPS Bioscience, USA) was purchased. The chromophore pair of 5-[(2'-aminoethyl)-amino] naphthalene sulfonic acid (Edans) and 4-[[4-(dimethylamino) phenyl] azo] benzoic acid (Dabcyl) is used in the real-time fluorometric turn-on assay system. An internally quenched 14-mer fluorogenic peptide (Dabcyl-KTSAVLQSGFRKME-Edans) is used for the Mpro assay. The Mpro substrate was dissolved in the assay buffer containing 50 mM Tris-HCl pH 7.5, 200 mM NaCl, 10% Glycerol, and 1 mM DTT to make a stock solution of 250 μM. The GC376 Mpro inhibitor #78013 (Selleckchem, USA) was used as a control to inhibit SARS-CoV-2 Mpro in the assay.

FRET-based Mpro proteolytic assay

The Mpro activity was measured on the various concentrations of substrates as below: the final concentration of 1 μM Mpro was reacted with the 0–40 μM concentrations of the substrate at 298 K with the Biotek Synergy HTX microplate reader (Biotek, USA) for excitation at 360/40 nm and emission at 460/40 nm in the black-bottomed microplates of 384 Ills (Greiner, Austria). The reaction progress was monitored until the fluorescence signals reached the plateau; at this point we deemed Mpro digested all the FRET substrates.

Calculations of solvent accessible surface area (SASA) of Mpro

The solvent-accessible surface area (SASA) is calculated by using the crystal structure of Mpro (PDB ID: 5R7Y) (22). The total SASA of a target is calculated with only the target molecule by omitting all other parts. The SASA of a target in Mpro dimer is calculated as the state bound with all other interacting parts. The interaction surface is calculated by deducting the SASA in dimer from the total SASA of a target. The SASA of targets is calculated by AREAIMOL in CCP4 (23).

The N-terminal ten amino acids peptide of Mpro

The N-terminal peptide of 10 amino acids of SGFRKMAFPS (N10) was synthesized by Peptron (Daejeon, South Korea) (Supplementary Fig. 2). The purity of synthesized peptides was confirmed in the Shimadzu prominence HPLC system as a single peak, and the mass analysis of the Shimadzu LCMS-2020 system verified the identification of the peptide sequence.

Inhibition assay

For the measurement of inhibition activity, 1 μM Mpro was incubated with the varying concentrations of the N-terminal peptide (N10: 0-500 μM) and the Mpro inhibitor (GC376: 0-100 μM) at 277 K for 30 minutes. After the incubation, 10 μM substrate was added at 298 K, and the reaction progress was monitored every minute for 3 hours. In the negative control, the assay was measured without Mpro. The control is measured with Mpro in the final volume containing 0.5% DMSO and 10 μM substrates showing the maximum fluorescence signal. The inhibitory activity of the compounds of N10 and GC376 was calculated by the following equation (17):

$$\%\ inhibition = 100\% - \left(\frac{FRET_{compound} - Negative_{control}}{Positive_{control} - Negative_{control}} \times 100\%\right)$$

ACKNOWLEDGEMENTS

This research was supported by a grant (22212MFDS254) from the Ministry of Food and Drug Safety and by the Bio & Medical Technology Development Program of the National Research Foundation of Korea (NRF) funded by the Ministry of Science and ICT (NRF-2017M3A9E4078017).

CONFLICTS OF INTEREST

The authors have no conflicting interests.

AUTHOR CONTRIBUTIONS

Investigation, Sunyu Song, Yeseul Kim, Kiwoong Kwak, Hyunmin Lee, Hyunjae Park, and Lin-Woo Kang; writing, Sunyu Song, Yeseul Kim, Kiwoong Kwak, Hyunmin Lee, and Lin-Woo Kang; funding acquisition, Young Bong Kim, Hee-Jung Lee, and Lin-Woo Kang. All authors have read and agreed to the published version of the manuscript.

REFERENCES

1. Woo PC, Lau SK, Lam CS et al (2012) Discovery of seven novel mammalian and avian coronaviruses in the genus deltacoronavirus supports bat coronaviruses as the gene source of alphacoronavirus and betacoronavirus and avian coronaviruses as the gene source of gammacoronavirus and deltacoronavirus. J Virol 86, 3995-4008
2. Zhu N, Zhang D, Wang W et al (2020) A novel Coronavirus from patients with pneumonia in China, 2019. N Engl J Med 382, 727-733
3. Dhama K, Khan S, Tiwari R et al (2020) Coronavirus Disease 2019-COVID-19. Clin Microbiol Rev 33, e00028-20
4. Ullrich S and Nitsche C (2020) The SARS-CoV-2 main protease as drug target. Bioorg Med Chem Lett 30, 127377
5. Seyed Hosseini E, Riahi Kashani N, Nikzad H, Azadbakht J, Hassani Bafrani H and Haddad Kashani H (2020) The novel coronavirus disease-2019 (COVID-19): mechanism

of action, detection and recent therapeutic strategies. Virology 551, 1-9
6. Tison GH, Avram R, Kuhar P et al (2020) Worldwide effect of COVID-19 on physical activity: a descriptive study. Ann Intern Med 173, 767-770
7. Mallah SI, Ghorab OK, Al-Salmi S et al (2021) COVID-19: breaking down a global health crisis. Ann Clin Microbiol Antimicrob 20, 35
8. Kim D, Lee JY, Yang JS, Kim JW, Kim VN and Chang H (2020) The architecture of SARS-CoV-2 transcriptome. Cell 181, 914-921 e910
9. Ullrich S and Nitsche C (2022) SARS-CoV-2 papain-like protease: structure, function and inhibition. Chembiochem 23, e202200327
10. Lu R, Zhao X, Li J et al (2020) Genomic characterisation and epidemiology of 2019 novel coronavirus: implications for virus origins and receptor binding. Lancet 395, 565-574
11. Zhou P, Yang XL, Wang XG et al (2020) A pneumonia outbreak associated with a new coronavirus of probable bat origin. Nature 579, 270-273
12. Stevens CS, Oguntuyo KY and Lee B (2021) Proteases and variants: context matters for SARS-CoV-2 entry assays. Curr Opin Virol 50, 49-58
13. Huff S, Kummetha IR, Tiwari SK et al (2022) Discovery and mechanism of SARS-CoV-2 main protease inhibitors. J Med Chem 65, 2866-2879
14. Banerjee R, Perera L and Tillekeratne LMV (2021) Potential SARS-CoV-2 main protease inhibitors. Drug Discov Today 26, 804-816
15. Noske GD, Song Y, Fernandes RS et al (2023) An in-solution snapshot of SARS-COV-2 main protease maturation process and inhibition. Nat Commun 14, 1545
16. Jiang Z, Feng B, Zhang Y et al (2023) Discovery of novel non-peptidic and non-covalent small-molecule 3CL. Signal Transduct Target Ther 8, 209
17. Ma C, Sacco MD, Hurst B et al (2020) Boceprevir, GC-376, and calpain inhibitors II, XII inhibit SARS-CoV-2 viral replication by targeting the viral main protease. Cell Res 30, 678-692
18. Magro P, Zanella I, Pescarolo M, Castelli F and Quiros-Roldan E (2021) Lopinavir/ritonavir: repurposing an old drug for HIV infection in COVID-19 treatment. Biomed J 44, 43-53
19. Li C, Teng X, Qi Y et al (2016) Conformational flexibility of a short loop near the active site of the SARS-3CLpro is essential to maintain catalytic activity. Sci Rep 6, 20918
20. Nashed NT, Aniana A, Ghirlando R, Chiliveri SC and Louis JM (2022) Modulation of the monomer-dimer equilibrium and catalytic activity of SARS-CoV-2 main protease by a transition-state analog inhibitor. Commun Biol 5, 160
21. Hsu WC, Chang HC, Chou CY, Tsai PJ, Lin PI and Chang GG (2005) Critical assessment of important regions in the subunit association and catalytic action of the severe acute respiratory syndrome coronavirus main protease. J Biol Chem 280, 22741-22748
22. Miltner N, Kalló G, Csősz É et al (2023) Identification of SARS-CoV-2 Main protease (Mpro) cleavage sites using two-dimensional electrophoresis and in silico cleavage site prediction. Int J Mol Sci 24, 3236
23. Vuong W, Khan MB, Fischer C et al (2020) Feline coronavirus drug inhibits the main protease of SARS-CoV-2 and blocks virus replication. Nat Commun 11, 1891
24. Liu H, Iketani S, Zask A et al (2022) Development of optimized drug-like small molecule inhibitors of the SARS-CoV-2 3CL protease for treatment of COVID-19. Nat Commun 13, 1-16
25. Fu L, Ye F, Feng Y et al (2020) Both Boceprevir and GC376 efficaciously inhibit SARS-CoV-2 by targeting its main protease. Nat Commun 11, 4417
26. Goyal B and Goyal D (2020) Targeting the dimerization of the main protease of coronaviruses: a potential broad-spectrum therapeutic strategy. ACS Comb Sci 22, 297-305
27. Geretti AM and Easterbrook P (2001) Antiretroviral resistance in clinical practice. Int J STD AIDS 12, 145-153
28. Vandyck K and Deval J (2021) Considerations for the discovery and development of 3-chymotrypsin-like cysteine protease inhibitors targeting SARS-CoV-2 infection. Curr Opin Virol 49, 36-40
29. Nashed NT, Aniana A, Ghirlando R, Chiliveri SC and Louis JM (2022) Modulation of the monomer-dimer equilibrium and catalytic activity of SARS-CoV-2 main protease by a transition-state analog inhibitor. Commun Biol 5, 160
30. Tzou PL, Tao K, Pond SLK and Shafer RW (2022) Coronavirus Resistance Database (CoV-RDB): SARS-CoV-2 susceptibility to monoclonal antibodies, convalescent plasma, and plasma from vaccinated persons. PLoS One 17, e0261045